Tunable drug release from blend poly(vinyl pyrrolidone)-ethyl cellulose nanofibers

V. Umayangana Godakanda,[1,2] Heyu Li,[1,3] Laura Alquezar,[1] Lixiang Zhao,[1] Li-Min Zhu,[3] Rohini de Silva,[2] K. M. Nalin de Silva,[2]* and Gareth R. Williams[1]*

[1] UCL School of Pharmacy, University College London, 29-39 Brunswick Square, London, WC1N 1AX, UK

[2] Department of Chemistry, University of Colombo, Colombo 00300, Sri Lanka

[3] College of Chemistry, Chemical Engineering and Biotechnology, Donghua University, Shanghai 201620, China

* Authors for correspondence. Tel: +91 (0) 714 406 276 (KMNdS); +44 (0) 207 753 5868 (GRW). Email: kmnd@chem.cmb.ac.lk (KMNdS); g.williams@ucl.ac.uk (GRW).

Abstract

The management of pain and inflammation arising from wounds is essential in obtaining effective healing rates. The application of a wound dressing loaded with an anti-inflammatory drug would enable both issues to be ameliorated, and the aim of this work was to fabricate such a dressing by electrospinning. Fibers comprising ethyl cellulose (EC) and poly(vinyl pyrrolidone) (PVP) loaded with naproxen (Nap) were developed to be used in the early stages of wound care. A family of PVP/EC/Nap systems was prepared by varying the PVP: EC ratio. In all cases, the products of electrospinning comprise non-woven mats of fibers which generally have smooth and cylindrical morphologies. The formulations exist as amorphous solid dispersions, and there appear to be intermolecular interactions between all three components. Adjusting the polymer ratios results in tunable drug release, and formulations have been produced which give zero-order drug release over 20 and 80h. The fiber mats generated in this work thus have great potential to be used as dressings for the treatment of wound pain and inflammation.

Keywords: Naproxen, wound dressing, electrospinning, poly(vinyl pyrrolidone), ethyl cellulose

1. Introduction

Pain arising from acute or chronic wounds has a highly detrimental impact on patients' quality of life (Moffatt et al., 2002). Wound healing is often delayed by poor pain management, which leads to stress and affects both the physical and psychological wellbeing of the patient (Moffatt et al., 2002; Woo 2012; Vinklárková et al., 2015). Further, a number of chemical mediators (e.g. serotonin, leukotrienes, histamine) are released from wounded tissues, and often lead to neurogenic inflammation and enhanced sensitivity to pain (Julius and Basbaum, 2001). To reduce inflammation arising from wounded tissue, non-steroidal anti-inflammatory drugs (NSAIDs) are often prescribed as they possess excellent analgesic activity and can bring about local pain relief if present at suitable concentrations at the wound site. This can be a challenge with systemic administration, but when applied topically NSAIDs can effectively relieve pain from wounds (Moffatt et al., 2002; Vinklárková et al., 2015; Yurdasiper et al., 2018).

Naproxen (Nap) is a NSAID which gives analgesic, antipyretic and anti-inflammatory effects through non-selective inhibition of the COX-1 and COX-2 enzymes. It is used to relieve inflammation, swelling, and joint pain (Üstünda et al., 2011; Attia, 2009). Nap is a Biopharmaceutical Classification System (BCS) class II drug, and hence its bioavailability is limited by its low propensity to dissolution (Allesø et al., 2009). In addition, the efficacy of oral naproxen is limited by adverse side effects, such as irritation and ulceration of the gastro-intestinal mucosa, nausea, and systemic toxicity (Huang et al., 2012; Bushra and Aslam, 2010). In the case of wounds, topical delivery of Nap can be used to avoid many of the side effects arising from the oral route. It can also extend the period of therapeutic action at the wound site (Üstünda et al., 2011). However, one major drawback in the topical application of drugs is the need to frequently remove and reapply the dressing or dosage form: such handling can significantly exacerbate acute wounds. A better solution would be to have a dressing

comprising a smart fabric giving sustained release over a prolonged period of time, thus eliminating the need for frequent changes in dressings and reducing inflammation during wound healing (Wang and Windbergs, 2011).

To prepare smart fabric dressings, electrospinning can be employed. This is a versatile method of preparing textiles with tunable properties, and is suitable for many applications (Wang and Windbergs, 2011; Frenot and Chronakis, 2013; Ramakrishna et al., 2006; Bhardwaj and Kundu, 2010; Farokhi et al., 2018). The primary components of the electrospinning apparatus consist of a syringe attached to a metal needle (the "spinneret"), a high voltage power supply, and a metal collector. A polymer solution is prepared in a volatile solvent, and loaded into a syringe. The solution is then ejected through the spinneret towards the collector at a controlled rate, with a high voltage applied between the two. This electric field causes repulsive charges to build up on the surface of the liquid droplet at the tip of the needle, deforming the droplet into a conical shape (the Taylor cone). The moment repulsive forces overcome the surface tension, a jet is ejected from the tip of the cone; this subsequently narrows as the jet approaches the collector, resulting in the deposition of a mat of solid fibers (typically with diameters on the nm scale) on the collector (Wang and Windbergs, 2011; Frenot and Chronakis, 2013; Ramakrishna et al., 2006; Ahmed et al., 2015).

Electrospun fiber mats have high surface area to volume ratios, high levels of porosity, and can incorporate high loadings of a functional component; this gives them applications in a number of fields including water filtration, catalysis, sensing, biomedical applications and drug delivery (Wang and Windbergs, 2011; Frenot and Chronakis, 2013; Ramakrishna et al., 2006; Bhardwaj and Kundu, 2010; Ahmed et al., 2015; Yu et al., 2013; Li et al., 2017; Kaassis et al., 2014; Quan et al., 2013; Tort et al., 2017; Kamble et al., 2017). While in the simplest experiment only a single solution is processed, resulting in monolithic fibers, it is also possible to work with multiple solutions at the same time, giving materials with core/shell or other nanoscale architectures (Heydari et al., 2018; Zhao et al.,

2005; Yang et al., 2017). Scale up of the process is also possible (Démuth et al., 2016). Electrospun fibers have been shown to have great potential in a range of areas of biomedicine, including wound healing. For instance, Kataria et al. (2014) reported an electrospun ciprofloxacin-loaded poly(vinyl alcohol) / sodium alginate formulation with high entrapment efficiency, extended drug release kinetics, and potent activity in an *in vivo* rabbit study. Electrospun fibers have clear potential for application in a range of settings in the clinic (Liu et al, 2018; Williams, Raimi-Abraham and Luo, 2018), and a Phase IIb clinical trial of an electrospun product for the treatment of mucosal lesions is currently underway (https://clinicaltrials.gov/ct2/show/NCT03592342).

Perhaps most commonly, electrospun fibers have been used to accelerate the dissolution of poorly water soluble drugs such as naproxen and ibuprofen (Yu et al., 2009). This can be very desirable to give rapid relief of symptoms, but often a more complex drug delivery profile is required. A drug delivery system (DDS) combining two polymers with different properties offers the potential to deliver novel and tunable drug release profiles even from a single fluid electrospinning process (Kaassis et al., 2014). Poly(vinylpyrrolidone) (PVP) is a US FDA approved biocompatible, non-toxic, fast dissolving polymer that is widely used in drug formulations (Koczkur et al., 2015; Illangakoon et al., 2014; Fischer and Bauer, 2009). It has been investigated extensively for the preparation of fast-dissolving electrospun materials containing for instance ibuprofen (Yu et al., 2009) or paracetamol and caffeine (Illangakoon et al., 2014). For extended release times, insoluble polymers are typically used. One such material is ethyl cellulose (EC), which has excellent biocompatibility and hydrophobic properties, leading to sustained drug release (Yu et al., 2013; Huang et al., 2012; Ahmad et al., 2013). Electrospun EC formulations have been prepared loaded with a number of drugs (e.g. ketoprofen) (Huang et al., 2012). PVP and EC have also been electrospun together in a coaxial experiment to give core-sheath fibers with tunable biphasic drug release properties (Yu et al., 2013).

In this work, we sought to use blends of PVP and EC to generate a family of electrospun fibers with tunable drug release, through incremental variation of the polymer mass ratios. Combining the two polymers both allows us to tune the drug release profile and also to produce fibers using a low viscosity (4 cP) EC solution. Although coaxial electrospinning of PVP and EC has been reported previously (Yu et al., 2013), this previous study used two separate solutions (one of EC, one of PVP) rather than a blend and a complex coaxial electrospinning process was required to generate fibers. The simple blend approach here is beneficial because it is much easier to scale up and translate to an industrial setting. The materials were loaded with naproxen, and characterized in terms of their morphology, physical form, and drug release properties. A wide range of drug release profiles are seen from the PVP/EC formulations, which therefore have potential to be used as smart dressings for the treatment of inflammation in early wound healing.

2. Experimental details

2.1 Materials

Polyvinylpyrrolidone (PVP; average molecular weight 360,000 Da), ethyl cellulose (EC; 48% ethoxy, 4 cP), and phosphate-buffered saline (PBS) were purchased from Sigma-Aldrich Ltd. Naproxen sodium was procured from Santa Cruz Biotechnology Inc. All other chemicals used were analytical grade, and water was doubly distilled before use.

2.2 Preparation of neutral naproxen

1 g of naproxen sodium was dissolved in 50 mL of 37% w/w aqueous HCl to convert the salt to its acid form. The precipitate was washed with distilled water until blue litmus paper showed no change in colour.

2.3 Preparation of electrospinning solutions

Solubility testing was initially carried out determine the most appropriate solvent in which to co-dissolve all three components of the fibers (PVP, EC, and naproxen [Nap]). Ethanol was found suitable for this, and thus selected for use owing to its low cost and low toxicity. PVP, EC and Nap were co-dissolved in ethanol under magnetic stirring for 12 h at room temperature, to yield clear and homogenous solutions with a total polymer concentration of 10% w/v and Nap concentration of 2.5% w/v. The w/w component ratio of PVP to EC was varied as shown in Table 1, and a series of spinning solutions prepared. Solution viscosity was measured using a Bohlin Gemini 150 rotational rheometer (Malvern) at a shear rate of 199.1 s^{-1}.

Table 1: Details of the electrospinning solutions and fibers prepared in this work.

Formulation	Solution			Fiber product			
	PVP:EC ratio (w/w)	Nap (% w/v)	Viscosity (Pa)[a]	PVP (% w/w)	EC (% w/w)	Nap (% w/w)	Surface tension (mN)[b]
F0	3:2	-	0.236	60	40	-	27.2 ± 0.7
PVP/EC(4:1)	4:1	2.5	0.298	64	16	20	13.8 ± 4.6
PVP/EC(3:2)	3:2	2.5	0.182	48	32	20	27.9 ± 1.0
PVP/EC(1:1)	1:1	2.5	0.220	40	40	20	28.2 ± 1.3
PVP/EC(2:3)	2:3	2.5	0.250	32	48	20	28.7 ± 1.5
PVP/EC(1:2)	1:2	2.5	0.159	26.7	53.3	20	27.0 ± 1.0
PVP/EC(1:4)	1:4	2.5	0.137	16	64	20	26.4 ± 0.7

[a] At a shear rate of 199.1 s^{-1}. [b] This refers to the tension between the fiber mat and the Kibron probe.

2.4 Electrospinning

The required solution was loaded into a 5.0 mL Terumo plastic syringe, which was attached to a metal spinneret (internal diameter 0.61 mm, 20G). A syringe pump (KDS100, Cole-Parmer) was used to dispense the solution at a flow rate of 1.0 mL/h. A FuG Elektronic HCP35-35000 power supply was employed to apply a voltage of 16 kV (selected after a series of optimization experiments) between the spinneret and a grounded collector located 20 cm away. The latter comprised a metal plate of 15 × 20 cm covered with aluminium foil. Spinning was conducted at room temperature (ca. 25 °C) for 5 h. The fiber mats produced were then removed from the collector and stored in a vacuum desiccator at room temperature to remove any residual solvent.

2.5 Fiber characterization

2.5.1 Morphology

The fibers were visualized using scanning electron microscopy (SEM) on a FEI Quanta 200F instrument. Prior to scanning, samples were gold sputtered to make them electrically conductive. The images obtained were analyzed using the ImageJ software (National Institutes of Health). The fiber diameters were measured at >100 locations for each sample to determine their mean size.

2.5.2 Surface properties, physical form, and component compatibility

Surface tension was determined using a Delta-8 instrument (Kibron), with samples measured at least 6 times. Differential scanning calorimetry (DSC) was carried out using a Q2000 instrument (TA Instruments). Samples were loaded into sealed and pin-holed Tzero pans, and heated from 40 to 200 °C at 10 °C min^{-1} under a flow of nitrogen (50 mL min^{-1}). X-ray diffraction (XRD) was undertaken on Stoe STADI-P diffractometer supplied with Mo $K\alpha_1$ radiation (0.7093Å; 50kV and 30mA). Patterns were collected over the 2θ range 2 to 30°. Fourier transform infrared (FTIR) spectroscopy was performed on a Perkin-Elmer Spectrum 100 instrument, over the range 650–4000 cm^{-1} at a resolution of 1 cm^{-1}. Surface

2.5.3 In vitro *drug release*

A sample of ca. 10 mg was cut from each fiber mat and enclosed in dialysis tubing (molecular weight cut-off 3,500 Da). The tubing was then sealed with plastic clips (Fig. 1). Once the dialysis bags are sealed inside the clips only one side of the mat surface is exposed to the release media, which goes some way towards mimicking release into a wound site. Each disk was immersed in 100 mL of PBS at pH 7.4 and stirred at 110 rpm and 37° C. Aliquots (2 mL) were removed at regular intervals and the release medium replenished with fresh preheated PBS. The Nap concentration in the aliquots was quantified by UV spectroscopy (UV-Cary 100 instrument) at 230 nm. Where necessary, dilution with

PBS) of the aliquots was carried out to obtain absorption values in the linear region of the calibration plot (0.2-0.7) absorption region. Experiments were performed in triplicate (n=3). A control experiment was carried out using 2 mg of Nap.

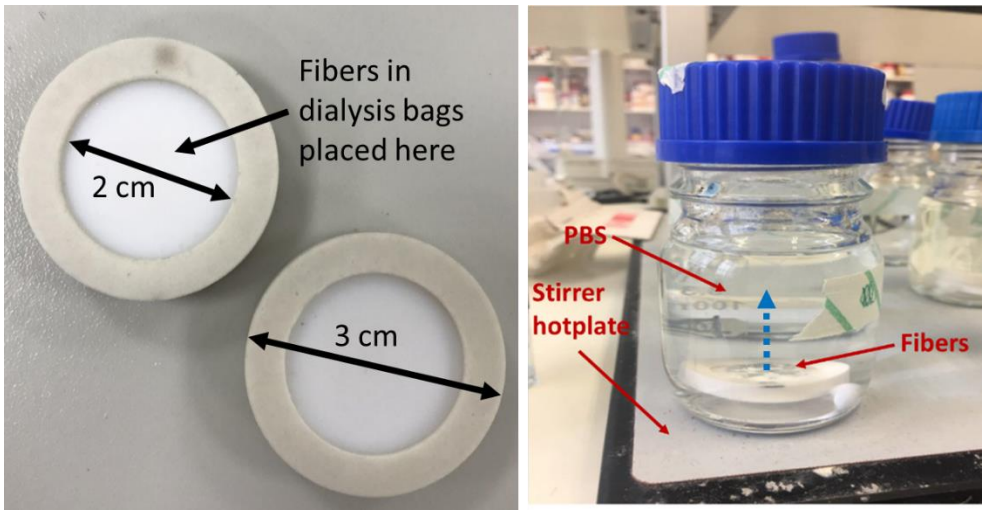

Fig. 1: Digital photographs of the dissolution discs used in this study. The image on the left shows the discs and their dimensions, and that on the right the complete release set-up. The dotted line on the right indiates the drug release direction.

3. Results and discussion

3.1 Fiber morphology and surface properties

Fibers were successfully produced in all cases, and in general have smooth and cylindrical morphologies (Fig. 2). The blank F0 formulation gave fibers with a rough surface, two apparent size populations, and a mean diameter of 412 ± 308 nm. The drug-loaded fiber series PVP/EC(4:1) to PVP/EC(1:4) showed gradual morphological changes with the variation of the PVP: EC ratio. The PVP/EC(4:1) formulation possesed a range of fiber diameters with the mean diameter lying at 647 ± 245 nm. Two distinct populations of fibers can be seen, one with much greater diameter than the other. When the PVP : EC ratio was reduced to 3:2 w/w the fibers showed more uniformity in their diameter (505 ± 171 nm), but there are wrinkles visible on the fiber surfaces. The PVP/EC(1:1) system (1:1 w/w ratio) appeared similar, but with more curvature noted and reduced wrinking. PVP/EC(1:1) has a slightly smaller diameter than PVP/EC(3:2) at 409 ± 89 nm. PVP/EC(2:3) showed two

significant fiber populations, similar to PVP/EC(4:1), and mean diameters of 497 ± 156 nm. The PVP/EC(1:2) fibers are smooth and cylindrical, with diameters of 542 ± 140 nm. PVP/EC(1:4) also contains smooth and cylindrical fibers, but with markedly higher diameters (802 ± 109 nm). There are also some small particles visible on the fiber surfaces. Overall, although it is clear that the polymer ratio does affect the fiber size and size uniformity, there are no clear trends in the data. It appears the solutions of medium viscosity give the narrowest fibers (Fig. S1, Supplementary Information).

The surface tension of the fibers was also determined (Table 1). Other than the PVP/EC(4:1) formulation, which has a markedly lower surface tension than the other samples owing to its very high PVP content, the values are essentially identical for all the samples.

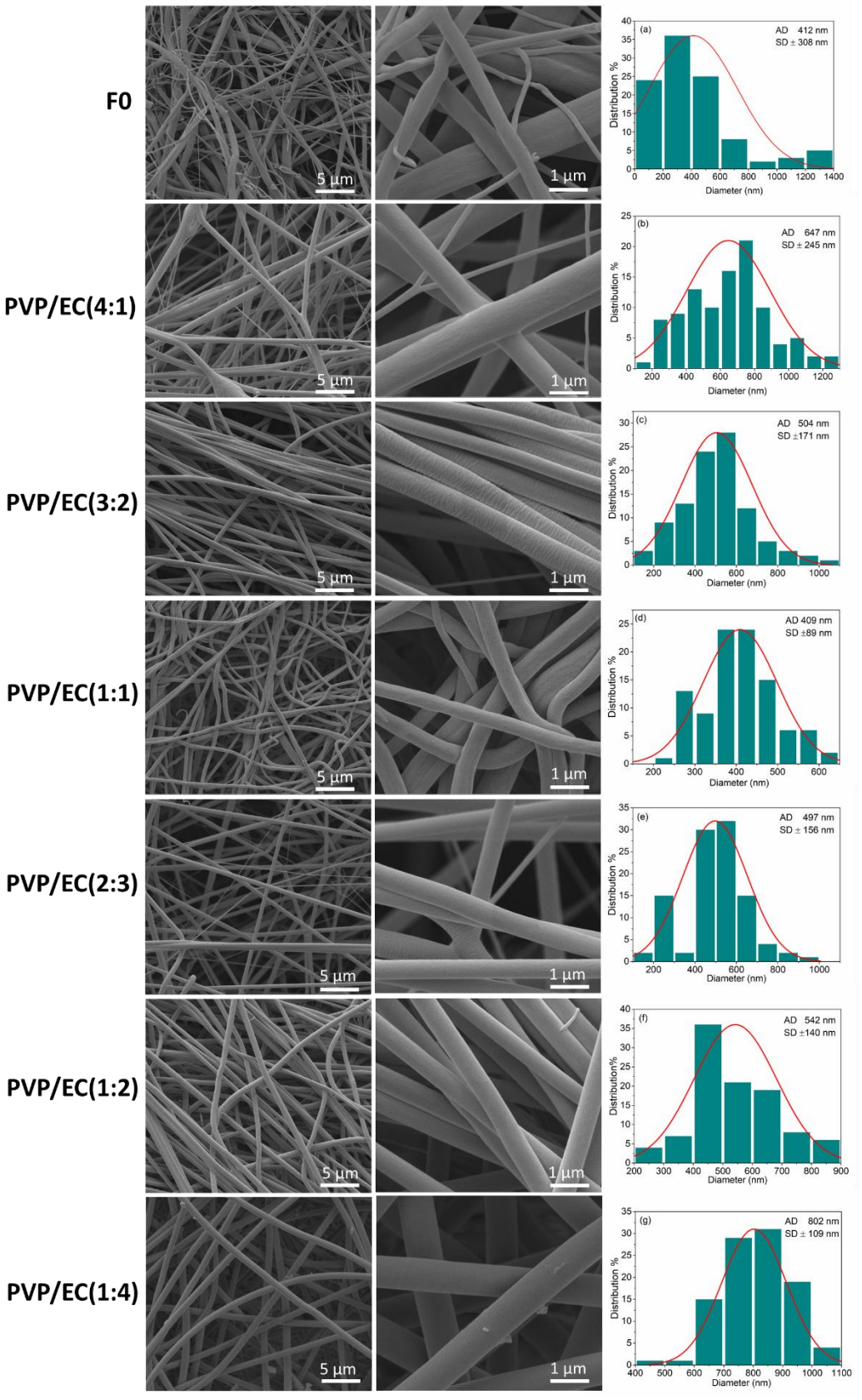

Fig. 2: SEM images of the PVP/EC/Nap nanofibers, together with their size distributions.

3.2 Physical form

DSC and XRD were employed to characterize the physical form of Nap in the six electrospun formulations. DSC thermograms are shown in Fig. 3a. The DSC thermogram of pure naproxen exhibits a sharp melting endotherm at 159.4 °C, in good agreement with the values reported for neutral naproxen in the literature (Hadi et al., 2014). The raw drug material is hence crystalline. Neither pure PVP nor EC show any fusion peaks or phase transitions in their DSC traces, indicating their amorphous nature. In the case of PVP, a broad endotherm arising from water loss can be seen ranging from ca. 50 to 150 ºC. Similarly to PVP, the fibers show only broad endotherms (between ca. 80 and 120 °C) consistent with water loss, and no melting events can be seen. This can be attributed to Nap being present in the amorphous form in the fibers (Yu et al., 2009; Yu et al., 2013). The glass transition temperature is not always clear, but in most of the systems there is a T_g visible between 150 and 175 °C (Fig. S2). The water loss endotherm can be seen to decline in intensity as the EC content of the fibers increases, and is much more obvious in the case of PVP/EC(4:1) than PVP/EC(1:4).

XRD patterns are presented in Fig. 3b. The pure Nap powder displays numerous sharp reflections in its pattern. This confirms the crystalline nature of the pure drug (Akduman et al., 2014). The diffraction patterns of PVP and EC comprise a diffuse background with broad halos and no Bragg diffraction. The neat polymers are therefore amorphous, as reported in the literature (Yu et al., 2013; Trivedi et al., 2015). The drug-free F0 fibers do not show any Bragg reflections, as expected given the amorphous nature of both constituent polymers. Similarly, the drug-loaded fibers PVP/EC(4:1) to PVP/EC(1:4) display only the broad haloes typical of amorphous materials. Therefore, it can be concluded that Nap is dispersed in the fibers in an amorphous state, which concurs with the DSC observations. Similar findings have been reported in several previous studies on electrospun formulations (Yu et al., 2009; Akduman et al., 2014). During electrospinning the solvent is evaporated at a rapid rate, leading to very quick solidification of the initial solution. This means that the Nap molecules do not have time during drying to organize themselves into the regular arrangement of a

crystal structure, and thus electrospinning generally gives amorphous products with random arrangements of molecules similar to that present in the solution state (Yu et al., 2013).

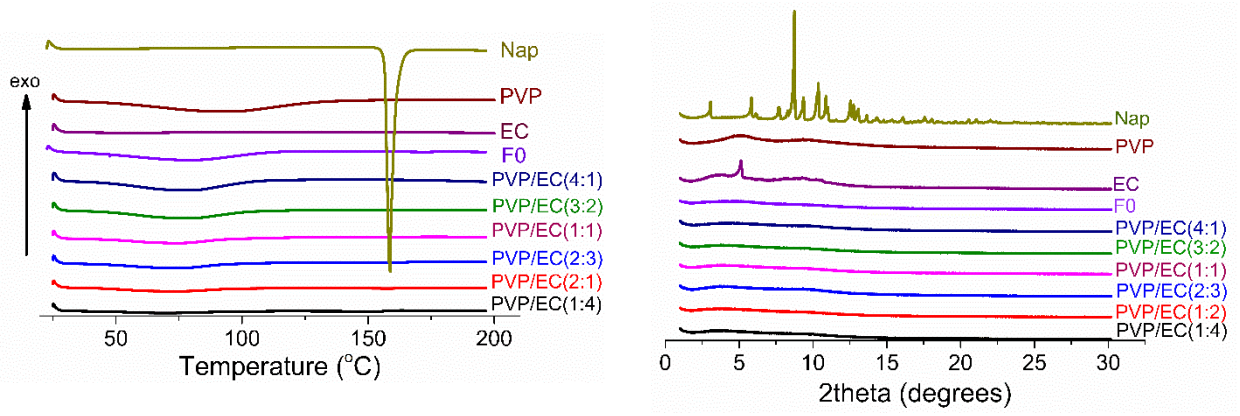

(a) **(b)**

Fig. 3: (a) DSC thermograms and **(b**) XRD patterns of the formulations and raw materials. The peak at 5° in the EC pattern is an artefact from the experimental set-up.

3.3 Component compatibility

To obtain high-quality and stable amorphous composites compatibility among the components (PVP, EC and Nap) is of crucial importance. This was investigated through FTIR analysis. The chemical structures of the components are given in Fig. 4. Nap, PVP and EC have free hydroxyl groups and carbonyl groups which can form proton donor-proton receptor interactions. Therefore, it can be assumed that hydrogen-bond interactions may occur within the Nap-loaded PVP/EC nanofiber formulations (Yu et al., 2013).

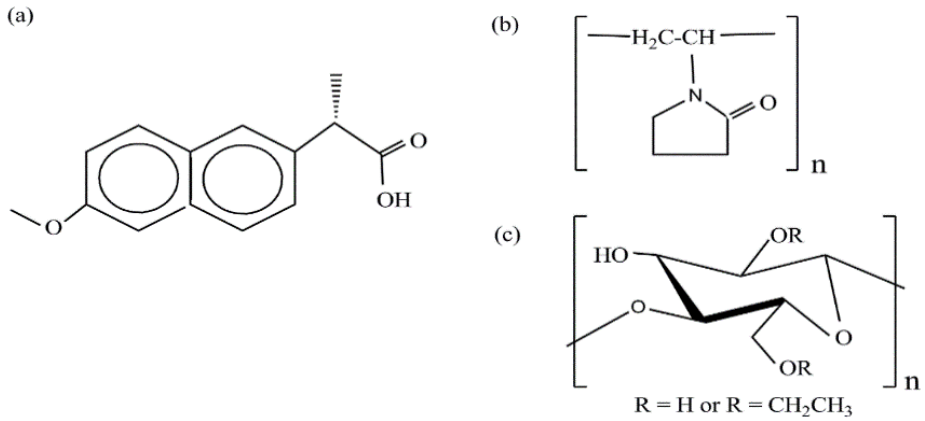

Fig. 4: Chemical structures of **(a)** Nap, **(b)** PVP, and **(c)** EC.

IR spectra are shown in Fig. 5. For blank PVP, the characteristic peaks of C=O and C-N stretching appear at 1651 and 1284 cm^{-1} respectively (Yu et al., 2009; Chen et al., 2012; Wang et al., 2013). EC

shows characteristic peaks at 1052 and 1375 cm^{-1}, indicating C-O-C stretching and -CH bending, respectively. Bands at 2972 and 2870 cm^{-1} arise from -CH stretching vibrations. These peaks are observed in all the fiber formulations without any significant changes in peak positions (Akduman et al., 2014). With the increase in EC content moving from PVP/EC(4:1) to PVP/EC(1:4), the intensity of the peak at 1052 cm^{-1} was observed to increase, while bands attributable to PVP (1660 – 1674 cm^{-1}) decline in intensity. The C=O peak of PVP increases in wavenumber (from 1658 – 1674 cm^{-1}) as the amount of EC in the system rises, which might indicate H-bonding between EC and PVP and/or PVP and Nap.

Nap has vibration bands at 1726 cm^{-1} from C=O stretching, at 1227 cm^{-1} from C–O–C- stretching, at 1394 cm^{-1} due to CH_3 bending, and at 1604 cm^{-1} from aromatic C=C vibrations (Hadi et al., 2014; Akduman et al., 2014; Hadi et al., 2015; Akbari et al, 2015). The C=O and C=C stretches of Nap are visible in the spectra of all the drug-loaded fibers, with slight shifts in position to 1606 cm^{-1} and 1723-1727 cm^{-1}. This both confirms the presence of Nap in the formulations and the likely presence of H-bonding interactions with the two polymers (Akduman et al., 2014).

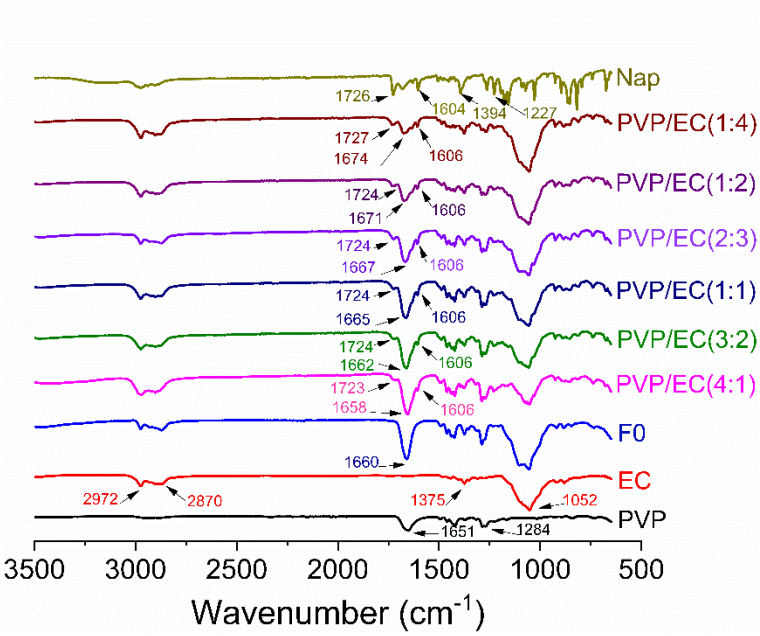

Fig. 5: FTIR spectra of the fibers and raw materials

3.5 In vitro *drug release*

Nap shows a UV absorbance peak at 230 nm when dissolved in PBS at pH 7.4. The amount of Nap released from the fibers was hence determined by UV spectroscopy, using a calibration curve A= 0.3381C + 0.014 (R^2 = 0.9956), where C is the concentration of Nap (mg/L), and A is the solution absorbance at 230 nm (linear range 0.6 – 2 mg/L). The *in vitro* drug release profiles of the six formulations are depicted in Fig. 6. A control experiment was performed using 2 mg of pure Nap, but no release was detected under these experimental conditions owing to its poor soolubility. It is clear that the fiber formulations offer clear advantages over the pure drug, accelerating release to give a range of profiles under the experimental conditions used in this work. While the pure drug could not usefully be applied to a wound site to yield a therapeutic effect, the fibers could.

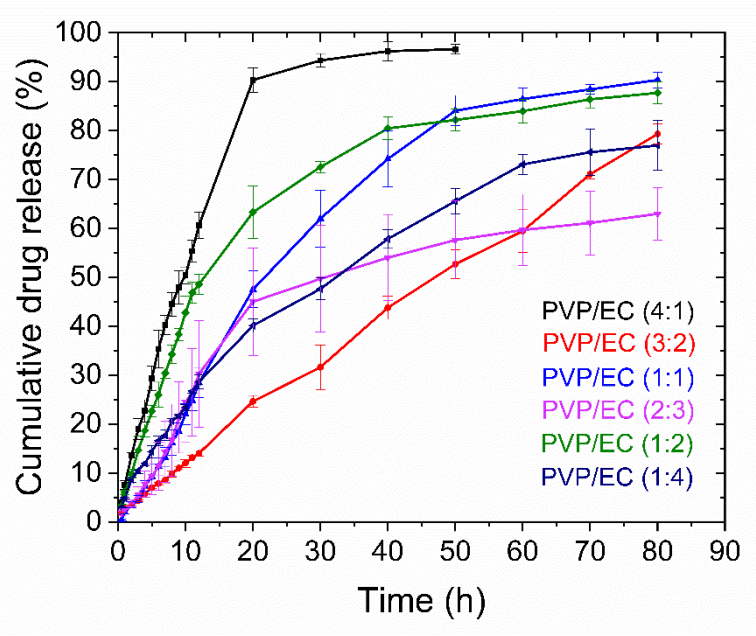

Fig. 6: *In vitro* drug release profiles. Data are shown as mean ± S.D. (n =3).

The PVP/EC(4:1) formulation, which has the highest PVP content, showed the fastest release of Nap (90% Nap released in the first 20 h). This can be ascribed to the hydrophilicity of PVP; when the content of EC was increased the release of Nap was retarded due to the hydrophobicity of EC. These results are in agreement with the findings of Huang et al. in their work with tri-layered PVP/EC meshes (Huang et al., 2012). However, it is clear from Fig. 6 that there is no clear trend in the data in terms of how drug release varies with the PVP/EC content. It is interesting though that two of the formulations provide approximately zero-order drug release profiles: PVP/EC(4:1) gives linear release over 20 h, while PVP/EC(3:2) gives linear release over 80 h. PVP/EC(4:1) might be useful in applications where Nap release is needed only for a short period (acute wounds), while PVP/EC(3:2) could be utilized for chronic wounds where administration of Nap might be required for a longer period of time. Zero order release has been seen previously from electrospun fibers, but only by using complicated multi-liquid processes such as triaxial and modified triaxial electrospinning (Yu et al., 2015; Yang et al., 2017). Here, we achieve such a release profile with a simple blend system, which will be much more amenable to industrial applications and scale-up.

The zero order model is defined by the equation

$$Q_t = Q_0 + k_0 t$$

where Q_t is the amount of drug dissolved in time t, Q_0 is the initial amount of drug in the solution (Q_0 = 0) and k_0 is the zero order release constant. The fits of the zero order model to PVP/EC(4:1) and PVP/EC(4:1) are summarized in Table 2, with the graphical plots in Fig. 7.

Table 2: Kinetic parameters calculated using the zero-order model.

Formulation	k_o (h^{-1})	R^2
PVP/EC(4:1)	5.01	0.9667
PVP/EC(3:2)	1.03	0.9935

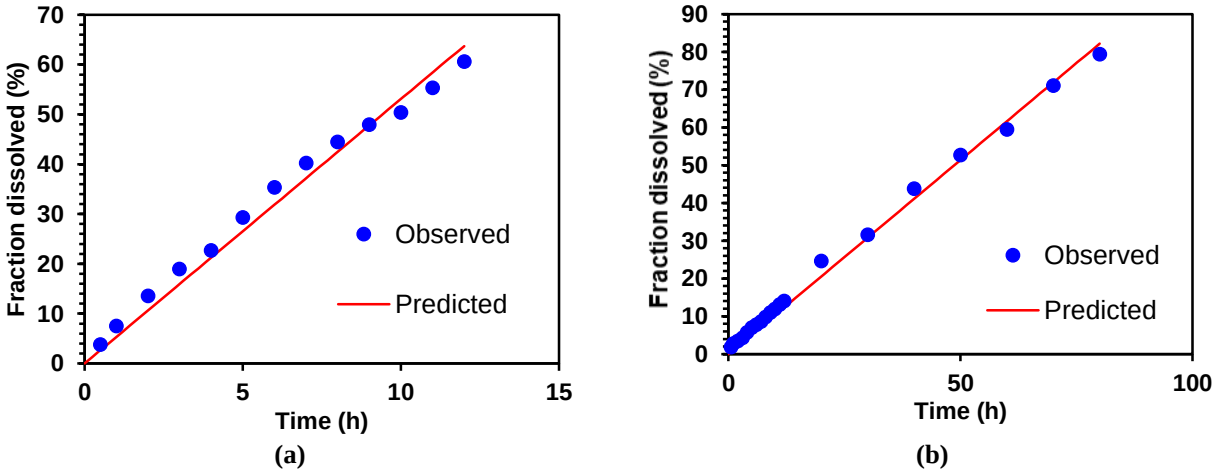

Fig. 7: Fits of the zero-order model to **(a)** PVP/EC(4:1) and **(b)** PVP/EC(3:2).

To gain further insight into the release mechanisms, SEM images were obtained of the fiber mats after the end of *in vitro* studies (Fig. 8).

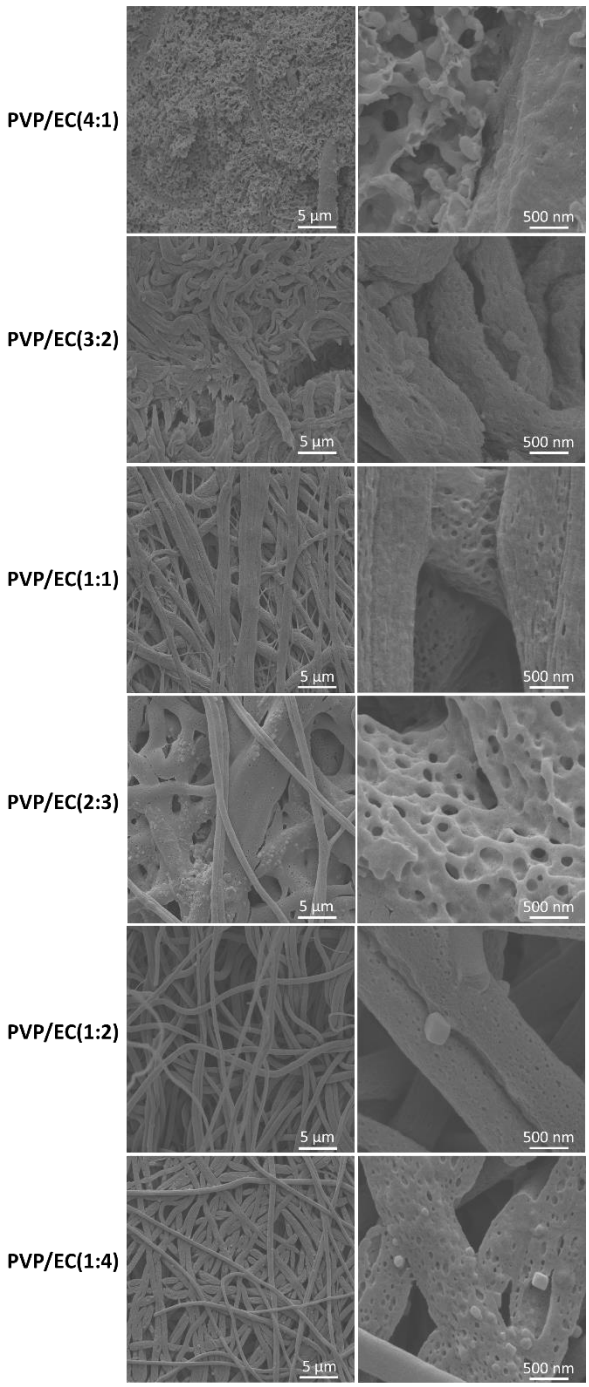

Fig. 8: The morphology of the fibers after *in vitro* drug release studies.

PVP is readily dissolved in water, as is apparent from all the SEM images in Fig. 8. The formulation with highest PVP content, PVP/EC(4:1), has completely lost its fibrous structure after drug release, and resembles an irregular film shape arising from the remaining (insoluble) EC. In all the other formulations, fibers can still be observed in the SEM images, but these have become porous as a result of the PVP dissolving and Nap being freed into the release medium. As the EC content rises, the fiber

morphology after drug release is increasingly clear, and while merging of fibers is visible for PVP/EC(3:2) and PVP/EC(1:1) individual fibers remain with the PVP/EC(1:4) material. There appear to be no clear correlations between the release profiles and the post-release fiber morphology. The images do however indicate there are different patterns of drug/polymer distribution in the different fibers. The residual material will comprise EC and any drug trapped within it. In the case of PVP/EC(3:2), there are large pores visible, suggesting that there were large areas of the fibers which were very PVP-rich and dissolved away. This might explain why there appear to be two distinct phases of release from this material: one rapid from the PVP-rich zones, and one slow from the EC zones. Some drug remains trapped in the EC regions of the fibers, which is why this system gives the lowest overall release percentage. Except for PVP/EC(4:1), the SEM images of the other fibers are more similar, showing evenly distributed but small pores. This might indicate a more homogeneous mixing of PVP and EC in these formulations.

4. Conclusions

Monoaxial electrospinning was used in this work to prepare blend nanofibers of poly(vinylpyrrolidone) (PVP) and ethyl cellulose (EC) loaded with naproxen. The fibers are generally found to be smooth and cylindrical, with diameters ranging from 647 to 802 nm. X-ray diffraction and differential scanning calorimetry verified that the fibers comprised amorphous solid dispersions, and IR spectra revealed the presence of intermolecular interactions between the polymers and drug. *In vitro* dissolution tests showed that it is possible to tune the drug release behavior of the fibers through the PVP: EC mass ratio, albeit not in a predictable fashion. Both the PVP/EC(4:1) and PVP/EC(3:2) formulations could provide zero order release profiles, the former over 20h and the latter over 80h. The fibers generated in this work thus have great potential in the treatment of pain and inflammation arising from wounds. Further, the EC/PVP system offers a simple platform which can be used to obtain tunable zero-order drug delivery systems, something which can usually only be achieved from much more complex formulation routes.

5. Acknowledgements

The authors gratefully thank the following for funding: the Royal Society International Exchanges Scheme (IE161184), the Engineering and Physical Sciences Research Council (EP/R512746/1), the UCL Global Engagement Fund, and the National Science Foundation of Sri Lanka (NSF/SCH/2018/02). We further thank Martin Vickers (UCL Chemistry) for assistance with XRD measurements, Andrew Weston (UCL School of Pharmacy) for the provision of SEM images, and Sarah Trenfield for her support with surface tension experiments.

6. References

Ahmad, B., Stoyanov, S., Pelan, E., Stride, E., Edirisinghe, M., 2013. Electrospinning of Ethyl Cellulose Fibres with Glass and Steel Needle Configurations. Food Res. Int. 54, 1761–1772.

Ahmed, F. E., Lalia, B. S., Hashaikeh, R., 2015. A Review on Electrospinning for Membrane Fabrication: Challenges and Applications. Desalination. 356, 15-30 .

Akduman, Ç., Özgüney, I., Kumbasar, E. P. A., 2104. Electrospun Thermoplastic Polyurethane Mats Containing Naproxen – Cyclodextrin Inclusion Complex. AUTEX Res. 14, 239–246.

Akbari, J., Enayatifard, R., Saeedi, M., Morteza-Semnani, K., Rajabi, S., 2015. Preparation, Characterization, and Dissolution Studies of Naproxen Solid Dispersions Using Polyethylene Glycol 6000 and Labrafil M2130. Pharm. Biomed. Res. 1, 44–53.

Al-deyab, S. S., El-Newehy, M. H., 2018. Fabrication of Electrospun Poly(Vinyl Alcohol)/Dextran Nanofibers via Emulsion Process as Drug Delivery System: Kinetics and in Vitro Release Study. Int. J. Biol. Macromol. 116, 1250-1259.

Allesø M., Chieng, N., Rehder, S., Rantanen, J., Rades, T., Aaltonen, J., 2009. Enhanced dissolution rate and synchronized release of drugs in binary systems through formulation: Amorphous naproxen-cimetidine mixtures prepared by mechanical activation. J. Control. Release. 136(1), 45-53.

Attia, D. A., 2009. In Vitro and in Vivo Evaluation of Transdermal Absorption of Naproxen Sodium. Aust. J. Basic Appl. Sci. 3 (3), 2154–2165.

Bhardwaj, N., Kundu, S. C., 2010. Electrospinning: A Fascinating Fiber Fabrication Technique. Biotechnol.Adv. 28, 325-47.

Bushra, R., Aslam, N., 2010. An Overview of Clinical Pharmacology of Ibuprofen. Oman Med. J. 25 (3), 155–1661.

Chen, M., Qu, H., Zhu, J., Luo, Z., Khasanov, A., Kucknoor, A. S., Haldolaarachchige, N., Young, D. P., Wei, S., Guo, Z., 2012. Magnetic Electrospun Fluorescent Polyvinylpyrrolidone Nanocomposite Fibers. Polym. 53, 4501–4511.

Démuth, B., Farkas, A., Pataki, H., Balogh, A., Szabó, B., Borbás, E., Sóti, P. L., Vigh, T., Kiserdei, É., Farkas, B., et al., 2016. Detailed Stability Investigation of Amorphous Solid Dispersions Prepared by Single-Needle and High Speed Electrospinning. Int. J. Pharm. 498, 234–

244.

Farokhi, M., Mottaghitalab, F., Fatahi, Y., Khademhosseini, A., Kaplan, D. L., 2018. Overview of Silk Fibroin Use in Wound Dressings. Trends Biotechnol. 36, 907–922.

Fischer, F., Bauer, S., 2009. Polyvinylpyrrolidon. Ein Tausendsassa in Der Chemie. Chemie Unserer Zeit 43, 376–383.

Frenot, A., Chronakis, I. S., 2003. Polymer Nanofibers Assembled by Electrospinning. Curr. Opin. Colloid Interface Sci. 8, 64–75.

Hadi, M. A., Rao, A. S., Rao, V. U., Sirisha, Y., 2014. Surface Response Methodology For Development and Optimization Of Naproxen Sustained Release Tablets. Asian J. Pharm. Clin. Res. 7, 125-133.

Hadi, M. A., Rao, N. G. R., Rao, A. S., 2015. Formulation and Evaluation of Ileo-Colonic Targeted Matrix-Mini-Tablets of Naproxen for Chronotherapeutic Treatment of Rheumatoid Arthritis Formulation and Evaluation of Ileo-Colonic Targeted Matrix-Mini-Tablets of Naproxen for Chronotherapeutic Treatment. Saudi Pharm. J. 24, 64-73.

Heydari, P., Varshosaz, J., Kharazi, A.Z., Karbasi, S., 2018. Preparation and Evaluation of Poly Glycerol Sebacate / Poly Hydroxy Butyrate Core - Shell Electrospun Nanofibers with Sequentially Release of Ciprofloxacin and Simvastatin in Wound Dressings. Polym. Adv. Tech. 29, 1795-1803.

Huang, G., Zhang, Z., 2012. Micro- and Nano-Carrier Mediated Intra-Articular Drug Delivery Systems for the Treatment of Osteoarthritis. J. Nanotechnol. 2012, 748909.

Huang, L. Y., Branford-White, C., Shen, X. X., Yu, D. G., Zhu, L. M., 2012. Time-Engineeringed Biphasic Drug Release by Electrospun Nanofiber Meshes. Int. J. Pharm. 436, 88–96.

Illangakoon, U. E., Gill, H., Shearman, G. C., Parhizkar, M., Mahalingam, S., Chatterton, N. P., Williams, G. R., 2014. Fast Dissolving Paracetamol/Caffeine Nanofibers Prepared by Electrospinning. Int. J. Pharm. 477, 369–379.

Illangakoon, U. E., Nazir, T., Williams, G. R., Chatterton, N. P., 2014. Mebeverine-Loaded Electrospun Nanofibers : Physicochemical Characterization and Dissolution Studies. J. Pharm. Sci. 103, 283–292.

Julius, D., Basbaum, A. I., 2001. Molecular Mechanisms of Nociception. Nature 413, 203-210.

Kaassis, A. Y. A., Young, N., Sano, N., Merchant, H. A., Yu, D.-G., Chatterton, N. P., Williams, G. R., 2014. Pulsatile Drug Release from Electrospun Poly(Ethylene Oxide)–sodium Alginate Blend Nanofibres. J. Mater. Chem. B 2, 1400-1407.

Kamble, P., Sadarani, B., Majumdar, A., Bhullar, S., 2017. Nanofiber Based Drug Delivery Systems for Skin : A Promising Therapeutic Approach. J. Drug Deliv. Sci. Technol. 41, 124–133.

Kataria, K., Gupta, A., Rath, G., Mathur, R.B., Dhakate, S.R., 2014. In vivo wound healing performance of drug loaded electrospun composite nanofibers transdermal patch. Int. J Pharm. 469(1), 102-110..

Koczkur, K. M., Mourdikoudis, S., Polavarapu, L., Skrabalak, S. E., 2015. Polyvinylpyrrolidone (PVP) in Nanoparticle Synthesis. Dalton Trans. 44 (41), 17883–17905.

Li, H., Williams, G. R., Wu, J., Lv, Y., Sun, X., Wu, H., Zhu, L., 2017. Thermosensitive Nanofibers Loaded with Ciprofloxacin as Antibacterial Wound Dressing Materials. Int. J. Pharm. 517, 135–147.

Liu, M., Zhang, Y., Sun, S., Khan, A.R., Ji, J., Yang, M., Zhai, G, 2018. Recent advances in electrospun for drug delivery purpose. J. Drug Targeting, DOI: 10.1080/1061186X.2018.1481413.

Moffatt, J, P. J. Franks, P.J., Hollinworth H., 2002. "Understanding Wound Pain and Trauma: An

International Perspective," in Pain at Wound Dressing Changes. European Wound Management Association (EWMA), pp 2–7.

Quan, J., Wu, C., Williams, G. R., Branford-White, C. J., Nie, H., Zhu, L., 2013. Novel Electrospun Nanofibers Incorporating Polymeric Prodrugs of Ketoprofen: Preparation, Characterization, and in Vitro Sustained Release. J. Appl. Polym. Sci. 130, 1570-1577.

Ramakrishna, S., Fujihara, K., Teo, W. E., Yong, T., Ma, Z., Ramaseshan, R., 2006. Electrospun Nanofibers: Solving Global Issues. Mater. Today. 9, 40-50 .

Tort, S., Acartürk, F., Be, A., 2017. Evaluation of Three-Layered Doxycycline-Collagen Loaded Nanofiber Wound Dressing. Int. J. Pharm. 529, 642–653.

Trivedi, M. K., Branton, A., Trivedi, D., Nayak, G., Mishra, R. K., Jana, S., 2015. Characterization of Physicochemical and Thermal Properties of Biofield Treated Ethyl Cellulose and Methyl Cellulose. Biomed. Mater. Res. 3, 83-91.

Üstünda, N., Apaydın, S., Karabay, Y.N.Ü., Yavaşoğlu, A., Karasulu H.Y., 2011. Evaluation of Skin Permeation and Anti-Inflammatory and Analgesic Effects of New Naproxen Microemulsion Formulations. Int. J. Pharm. 416, 136–144.

Vinklárková, L., Masteiková, R., Vetchý, D., Doledel, P., Bernatonien, J., 2015. Formulation of Novel Layered Sodium Carboxymethylcellulose Film Wound Dressings with Ibuprofen for Alleviating Wound Pain. Biomed. Res. Int. 2015, 892671.

Wang, B., Zhang, P.-P., Williams, G.R., Branford-White C.B.W., Quan, J., Nie, H.-L., Zhu, L.-M., 2013. A Simple Route to Form Magnetic Chitosan Nanoparticles from Coaxial-Electrospun Composite Nanofibers. J. Mater. Sci. 48, 3991-3998.

Wang, J., Windbergs, M., 2017. Functional Electrospun Fibers for the Treatment of Human Skin Wounds. Eur. J. Pharm. Biopharm. 119, 283–299.

Williams, G.R., Raimi-Abraham, B.T., Luo, C.J. Nanofibres in drug delivery. UCL Press, London, 2018.

Woo, K. Y., 2012. Exploring the Effects of Pain and Stress on Wound Healing. Adv. Ski. Wound Care 25, 38–44.

Yang, G. Z., Li, J. J., Yu, D. G., He, M. F., Yang, J. H., Williams, G. R., 2017. Nanosized Sustained-Release Drug Depots Fabricated Using Modified Tri-Axial Electrospinning. Acta Biomater. 53, 233–241.

Yu, D. G., Zhang, X. F., Shen, X. X., Brandford-White, C., Zhu, L. M., 2009. Ultrafine Ibuprofen-Loaded Polyvinylpyrrolidone Fiber Mats Using Electrospinning. Polym. Int. 58, 1010–1013.

Yu, D. G., Wang, X., Li, X. Y., Chian, W., Li, Y., Liao, Y. Z., 2013. Electrospun Biphasic Drug Release Polyvinylpyrrolidone / Ethyl Cellulose Core / Sheath Nanofibers. Acta Biomater. 9, 5665–5672.

Yu, D.G., Li, X.Y., Wang, X., Yang, J.H., Bligh, S.W.A., Williams, G.R., 2015. Nanofibers Fabricated Using Triaxial Electrospinning as Zero Order Drug Delivery Systems. ACS Appl. Mater. Interfaces 7, 18891-18897

Yurdasiper, A., Ertan, G., Heard, C. M., 2018. Enhanced Delivery Of Naproxen to the Viable Epidermis from an Activated Poly N-Isopropylacrylamide (PNIPAM) Nanogel: Skin Penetration, Modulation Of COX-2 Expression And Rat Paw Oedema. Nanomed. Nanotechnol., Biol. Med. 14, 2051-2059.

Zhao, W., Gu, J., Zhang, L., Chen, H., Shi, J., 2005. Fabrication of Uniform Magnetic Nanocomposite Spheres with a Magnetic Core/Mesoporous Silica Shell Structure. J. Am. Chem. Soc. 127 (25), 8916–8917.